



Published in final edited form as:

ACS Macro Lett. 2018 June 19; 7(6): 662–666. doi:10.1021/acsmacrolett.8b00281.

N,N-Diaryl Dihydrophenazines as Photoredox Catalysts for PET-RAFT and Sequential PET-RAFT/O-ATRP

Jordan C. Theriot^{†,‡}, Garret M. Miyake^{*,‡}, and Cyrille A. Boyer^{*,†}

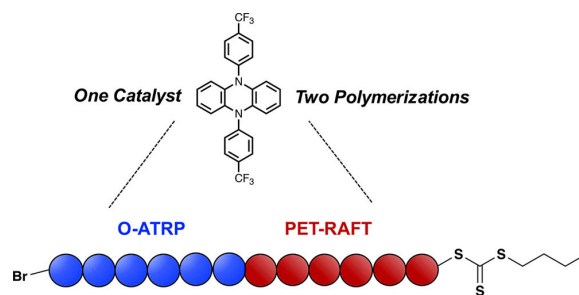
[†]Centre for Advanced Macromolecular Design (CAMD) and Australian Centre for Nanomedicine (ACN), School of Chemical Engineering, UNSW Australia, Sydney, NSW 2052, Australia

[‡]Department of Chemistry, Colorado State University, Fort Collins, Colorado 80523, United States

Abstract

N,N-Diaryl dihydrophenazines are employed as organic photoredox catalysts (PCs) for photoinduced electron/energy transfer–reversible addition–fragmentation chain transfer (PET-RAFT) polymerization. The ability of these PCs to mediate PET-RAFT is heavily dependent on the ability of the PC to access a photoexcited intramolecular charge transfer state. The use of PCs displaying intramolecular charge transfer in the excited state allows for efficient PET-RAFT of a variety of monomers, including vinyl acetate, and in a wide range of solvents. The ability of these PCs to also mediate organocatalyzed atom transfer radical polymerization (O-ATRP) is exploited to perform a sequential PET-RAFT/O-ATRP block copolymerization of PMA-*b*-PMMA using the same PC for both polymerizations.

Abstract



The use of photocatalysis^{1–7} has allowed for the introduction of light-controlled photoredox-mediated variants of many controlled radical polymerizations (CRPs), including two of the most well-known CRPs, reversible addition–fragmentation chain transfer (RAFT) polymerization,^{8–12} and atom transfer radical polymerization (ATRP).^{13–17} Initial

*Corresponding Authors garret.miyake@colostate.edu. cboyer@unsw.edu.au .

ASSOCIATED CONTENT

Supporting Information

The Supporting Information is available free of charge on the ACS Publications website at DOI: 10.1021/acsmacrolett.8b00281. Materials, methods, synthesis, characterization, and additional polymerization results (PDF)

Notes

The authors declare no competing financial interest.

development of these photoredox-catalyzed variants involved the use of a transition metal based photocatalyst (PC), such as tris(bipyridine)ruthenium(II) chloride [Ru(bpy)₃] or tris(2-phenylpyridinato-C²,N)iridium(III) [*fac*-Ir(ppy)₃]. However, in order to eliminate the potential for metal contamination in the polymeric product, organic PCs have been sought to replace these transition metal photocatalysts.¹⁸ In the case of photoinduced electron/energy transfer RAFT (PET-RAFT) polymerization, organic molecules such as eosin Y and pheophorbide A have been reported to efficiently mediate the polymerization of methacrylates and acrylates,^{19–21} and a phenothiazine derivative has been reported for the polymerization of acrylates and acrylamides.²²

In the case of photoredox-mediated ATRP, a number of PC types have been employed in organocatalyzed ATRP (O-ATRP).^{23–25} Among these, *N,N*-diaryl dihydrophenazines have emerged as highly promising PCs for O-ATRP due in part to their strong reducing power in their triplet excited state [$E^0(^2PC^{*+}/^3PC^*) < -2.0$ V vs SCE] and their ability to access an intramolecular charge transfer (CT) excited state upon photoexcitation with visible light. This intramolecular CT state is characterized by the transfer of the excited electron from the phenazine core to the *N*-aryl substituent, and the ability to access an intramolecular CT state has been shown to be a crucial aspect of efficient O-ATRP by these catalysts.^{26–28} Given the similarity of the role of the PC as an electron-transfer agent in both PET-RAFT and O-ATRP (Figure 1), we hypothesized that the same physical properties which make *N,N*-diaryl dihydrophenazines successful PCs for O-ATRP would also extend to the PET-RAFT process.

To begin, we sought to address whether or not *N,N*-diaryl dihydrophenazines are generally capable of serving as PCs for PET-RAFT. Two representative PCs, one exhibiting CT (PC **1**) and one without CT (PC **4**), were tested in the PET-RAFT polymerization of a number of different monomers using 460 nm blue LED as the light source (Table 1). PC **1** proved to be an efficient catalyst for the PET-RAFT of methyl acrylate (MA), methyl methacrylate (MMA), vinyl acetate (VAc), and *N,N*-dimethyl acrylamide (DMA). All of the polymers produced were of low dispersity (\bar{M}_w/\bar{M}_n , determined by GPC), and experimental and theoretical molecular weights (MWs) were in relatively good agreement. Notably, this is the first reported PET-RAFT polymerization of VAc by an organic PC. In contrast, PC **4** showed low or no conversion for all of the tested monomers.

For the polymerization of MA with PC **1**, control experiments were performed in which each of the polymerization components was removed, which resulted in no conversion in the absence of light or low conversion when PC was removed, indicating the potential for self-initiation of the RAFT agent under polymerization conditions (SI, Table S1).^{29–31} The absence of RAFT agent results in an uncontrolled polymerization, as demonstrated by high MW and \bar{M}_w/\bar{M}_n . To lend support to a PET-RAFT mechanism, ¹H NMR and MALDI-TOF analysis of a sample of PMA confirmed the presence of BTPA end groups (SI, Figures S2 and S3). Additionally, a sample of PMA was employed as a macro-initiator and efficiently chain extended in the presence of MA to yield PMA-*b*-PMA polymer, which is demonstrated by the shift in MW distribution after chain extension (SI, Figure S4).

In order to further investigate the behavior of these PCs as PET-RAFT catalysts, 6 *N,N*-diaryl dihydrophenazine PCs (3 with CT and 3 without CT) were employed in the PET-RAFT polymerization of MA in 6 different solvents (DMSO, DMF, DMAc, EtOAc, THF, and dioxane) under 460 nm blue LED light (Table 2). PCs **1–3** are capable of mediating the PET-RAFT of MA to high monomer conversion with low α and good agreement between theoretical and experimental MWs in solvents with a wide range of polarities. However, PCs **4–6** gave low or no monomer conversion within 6 h in all of the solvents tested.

The PET-RAFT polymerization of MA in DMSO using each of the 6 PCs was also monitored over time (Figure 2, see SI for additional experimental details). These data show that polymerizations using non-CT PCs as the catalyst present very low polymerization rates compared to those using CT PCs (k_{app} of PCs **4–6** is approximately three times slower than k_{app} of PCs **1–3**). Regardless of the CT nature of the PC, the polymerizations showed first-order kinetics with respect to monomer concentration, a linear growth of M_n with respect to conversion, and decrease in α with increasing monomer conversion (Figure 2 and SI, Figure S5). These data indicate that both types of PCs are able to participate in the PET-RAFT process. However, we hypothesize that the presence of intramolecular CT in the excited state allows PCs **1–3** to more efficiently participate in the electron transfer step needed to activate the RAFT agent. Similar to our previous observations regarding the behavior of these PCs in O-ATRP, the presence of intramolecular CT, and the resulting localization of the excited electron on the *N*-aryl substituent of the PC, may minimize the potential for unproductive back electron transfer, resulting in more efficient activation and overall faster PET-RAFT polymerizations. One key difference between the two polymerization types, however, is that to produce polymers with low α O-ATRP requires a higher PC concentration, typically 500 ppm, whereas PET-RAFT of MMA requires a significantly lower PC concentration (typically 10 ppm) (SI, Table S2).

With this information in hand, we sought to exploit the ability of PC **1** to efficiently catalyze both PET-RAFT and O-ATRP at different PC concentrations to devise an orthogonal copolymerization in which one PC is used to perform both types of CRPs in sequence. We began by synthesizing a dual initiator, EtBriB–BTPA, which contains a PET-RAFT initiating trithiocarbonate moiety and an O-ATRP initiating alkyl bromide moiety (Figure 3A). In the first stage of the copolymerization, MA was polymerized via PET-RAFT using PC **1** as the catalyst at 50 ppm. ^1H NMR of the PMA product indicates that the polymerization was controlled by the trithiocarbonate moiety of EtBriB–BTPA, and the alkyl bromide moiety was left unreacted as demonstrated by the presence of a methyl signal at 1.8 ppm (Figure 3B and SI, Figure S11). Subsequently, to form the second block, MMA was added, and the PC was increased to 500 ppm. The PMMA block is expected to selectively polymerize via O-ATRP as the BTPA moiety cannot polymerize methacrylates.³² GPC analysis revealed a shift in the retention time after chain extension, supporting the synthesis of PMA-*b*-PMMA (Figure 3C).

In conclusion, *N,N*-diaryl dihydrophenazines, previously employed as PCs for O-ATRP, were investigated for their ability to serve as photocatalysts for PET-RAFT polymerization. It was found that those PCs which possess an excited state with intramolecular CT character are able to efficiently polymerize a number of classes of monomers, including the first report

of a PET-RAFT polymerization of VAc by an organic PC. Additionally, it was found that all of the CT PCs tested resulted in efficient polymerization of MA in solvents with a wide range of polarities. Kinetic analysis indicated that non-CT PCs are also capable of mediating the PET-RAFT of MA. However, these polymerizations are slow compared to those which use a CT PC, likely due to less efficient activation. Finally, the ability of this one class of PCs to mediate two different controlled radical polymerizations was exploited to form a PMA-*b*-PMMA copolymer using both PET-RAFT and O-ATRP in sequence.

Supplementary Material

Refer to Web version on PubMed Central for supplementary material.

ACKNOWLEDGMENTS

This work was supported by Colorado State University. Research reported in this publication was supported by the National Institute of General Medical Sciences (Award Number R35GM119702) of the National Institutes of Health. The content is solely the responsibility of the authors and does not necessarily represent the official views of the National Institutes of Health. JCT acknowledges a National Science Foundation Graduate Research Fellowship Program (NSF-GRFP) fellowship, as well as additional funding for this collaboration from the National Science Foundation Graduate Research Opportunities Worldwide (NSF-GROW) program. We thank Matt Ryan for the donation of PC 2 and Bonnie Buss for the donation of PC 3. ARC Future Fellowship (FT12010096).

REFERENCES

- (1). Prier CK Rankic DA MacMillan DWC Visible Light Photoredox Catalysis with Transition Metal Complexes: Applications in Organic Synthesis *Chem. Rev* 2013 113 7 5322–5363 [PubMed: 23509883]
- (2). Shaw MH Twilton J MacMillan DWC Photoredox Catalysis in Organic Chemistry *J. Org. Chem* 2016 81 16 6898–6926 [PubMed: 27477076]
- (3). Corrigan N Shanmugam S Xu J Boyer C Photocatalysis in Organic and Polymer Synthesis *Chem. Soc. Rev* 2016 45 22 6165–6212 [PubMed: 27819094]
- (4). Yoon TP Ischay MA Du J Visible Light Photocatalysis as a Greener Approach to Photochemical Synthesis *Nat. Chem* 2010 2 7 527–532 [PubMed: 20571569]
- (5). Tucker JW Stephenson CRJ Shining Light on Photoredox Catalysis: Theory and Synthetic Applications *J. Org. Chem* 2012 77 4 1617–1622 [PubMed: 22283525]
- (6). Ohtsuki A Goto A Kaji H Visible-Light-Induced Reversible Complexation Mediated Living Radical Polymerization of Methacrylates with Organic Catalysts *Macromolecules* 2013 46 1 96–102
- (7). Ohtsuki A Lei L Tanishima M Goto A Kaji H Photocontrolled Organocatalyzed Living Radical Polymerization Feasible over a Wide Range of Wavelengths *J. Am. Chem. Soc* 2015 137 16 5610–5617 [PubMed: 25879620]
- (8). Xu J Jung K Atme A Shanmugam S Boyer C A Robust and Versatile Photoinduced Living Polymerization of Conjugated and Unconjugated Monomers and Its Oxygen Tolerance *J. Am. Chem. Soc* 2014 136 14 5508–5519 [PubMed: 24689993]
- (9). Xu J Jung K Boyer C Oxygen Tolerance Study of Photoinduced Electron Transfer–Reversible Addition–Fragmentation Chain Transfer (PET-RAFT) Polymerization Mediated by Ru(Bpy)₃Cl₂ *Macromolecules* 2014 47 13 4217–4229
- (10). Shanmugam S Xu J Boyer C Photoinduced Electron Transfer–Reversible Addition–Fragmentation Chain Transfer (PET-RAFT) Polymerization of Vinyl Acetate and *N*-Vinylpyrrolidinone: Kinetic and Oxygen Tolerance Study *Macromolecules* 2014 47 15 4930–4942
- (11). Shanmugam S Xu J Boyer C Light-Regulated Polymerization under Near-Infrared/Far-Red Irradiation Catalyzed by Bacteriochlorophyll *Angew. Chem., Int. Ed* 2016 55 3 1036–1040

- (12). Shanmugam S Xu J Boyer C Utilizing the Electron Transfer Mechanism of Chlorophyll a under Light for Controlled Radical Polymerization Chem. Sci 2015 6 2 1341–1349 [PubMed: 29560221]
- (13). Zhang G Song IY Ahn KH Park T Choi W Free Radical Polymerization Initiated and Controlled by Visible Light Photocatalysis at Ambient Temperature Macromolecules 2011 44 19 7594–7599
- (14). Liu X Zhang L Cheng Z Zhu X Metal-Free Photoinduced Electron Transfer–atom Transfer Radical Polymerization (PET–ATRP) via a Visible Light Organic Photocatalyst Polym. Chem 2016 7 3 689–700
- (15). Fors BP Hawker CJ Control of a Living Radical Polymerization of Methacrylates by Light Angew. Chem., Int. Ed 2012 51 35 8850–8853
- (16). Ma W Chen H Ma Y Zhao C Yang W Visible-Light-Induced Controlled Polymerization of Hydrophilic Monomers with Ir(Ppy)₃ as a Photoredox Catalyst in Anisole Macromol. Chem. Phys 2014 215 10 1012–1021
- (17). Treat NJ Fors BP Kramer JW Christianson M Chiu C-Y Read de Alaniz J Hawker CJ Controlled Radical Polymerization of Acrylates Regulated by Visible Light ACS Macro Lett 2014 3 6 580–584
- (18). Shanmugam S, Boyer C. Organic Photocatalysts for Cleaner Polymer Synthesis. Science. 2016; 352(6289):1053. [PubMed: 27230364]
- (19). Xu J Shanmugam S Duong HT Boyer C Organo-Photocatalysts for Photoinduced Electron Transfer-Reversible Addition–fragmentation Chain Transfer (PET-RAFT) Polymerization Polym. Chem 2015 6 31 5615–5624
- (20). Xu J Shanmugam S Boyer C Organic Electron Donor–Acceptor Photoredox Catalysts: Enhanced Catalytic Efficiency toward Controlled Radical Polymerization ACS Macro Lett 2015 4 9 926–932
- (21). Xu J Shanmugam S Fu C Aguey-Zinsou K-F Boyer C Selective Photoactivation: From a Single Unit Monomer Insertion Reaction to Controlled Polymer Architectures J. Am. Chem. Soc 2016 138 9 3094–3106 [PubMed: 26914442]
- (22). Chen M MacLeod MJ Johnson JA Visible-Light-Controlled Living Radical Polymerization from a Trithiocarbonate Iniferter Mediated by an Organic Photoredox Catalyst ACS Macro Lett 2015 4 5 566–569
- (23). Theriot JC, McCarthy BG, Lim C-H, Miyake GM. Organocatalyzed Atom Transfer Radical Polymerization: Perspectives on Catalyst Design and Performance. Macromol. Rapid Commun. 2017; 38(13):1700040.
- (24). Miyake GM Theriot JC Perylene as an Organic Photocatalyst for the Radical Polymerization of Functionalized Vinyl Monomers through Oxidative Quenching with Alkyl Bromides and Visible Light Macromolecules 2014 47 23 8255–8261
- (25). Treat NJ Sprafke H Kramer JW Clark PG Barton BE Read de Alaniz J Fors BP Hawker CJ Metal-Free Atom Transfer Radical Polymerization J. Am. Chem. Soc 2014 136 45 16096–16101 [PubMed: 25360628]
- (26). Theriot JC, Lim C-H, Yang H, Ryan MD, Musgrave CB, Miyake GM. Organocatalyzed Atom Transfer Radical Polymerization Driven by Visible Light. Science. 2016; 352(6289):1082. [PubMed: 27033549]
- (27). Lim C-H Ryan MD McCarthy BG Theriot JC Sartor SM Damrauer NH Musgrave CB Miyake GM Intramolecular Charge Transfer and Ion Pairing in *N,N*-Diaryl Dihydrophenazine Photoredox Catalysts for Efficient Organocatalyzed Atom Transfer Radical Polymerization J. Am. Chem. Soc 2017 139 1 348–355 [PubMed: 27973788]
- (28). Ryan MD Theriot JC Lim C-H Yang H Lockwood A Garrison NG Lincoln SR Musgrave CB Miyake GM Solvent Effects on the Intramolecular Charge Transfer Character of *N,N*-Diaryl Dihydrophenazine Catalysts for Organocatalyzed Atom Transfer Radical Polymerization J. Polym. Sci., Part A: Polym. Chem 2017 55 18 3017–3027
- (29). McKenzie TG Costa L. P. da M. Fu Q Dunstan DE Qiao GG Investigation into the Photolytic Stability of RAFT Agents and the Implications for Photopolymerization Reactions Polym. Chem 2016 7 25 4246–4253

- (30). McKenzie TG Fu Q Wong EHH Dunstan DE Qiao GG Visible Light Mediated Controlled Radical Polymerization in the Absence of Exogenous Radical Sources or Catalysts *Macromolecules* 2015 48 12 3864–3872
- (31). Xu J Shanmugam S Corrigan NA Boyer C Matyjaszewski K Sumerlin BS Tsarevsky NV Chiefari J Catalyst-Free Visible Light-Induced RAFT Photopolymerization Controlled Radical Polymerization: Mechanisms 2015 1187 247–267 American Chemical Society, Series Ed.; American Chemical Society Washington, DC
- (32). Keddie DJ Moad G Rizzardo E Thang SH RAFT Agent Design and Synthesis *Macromolecules* 2012 45 13 5321–5342

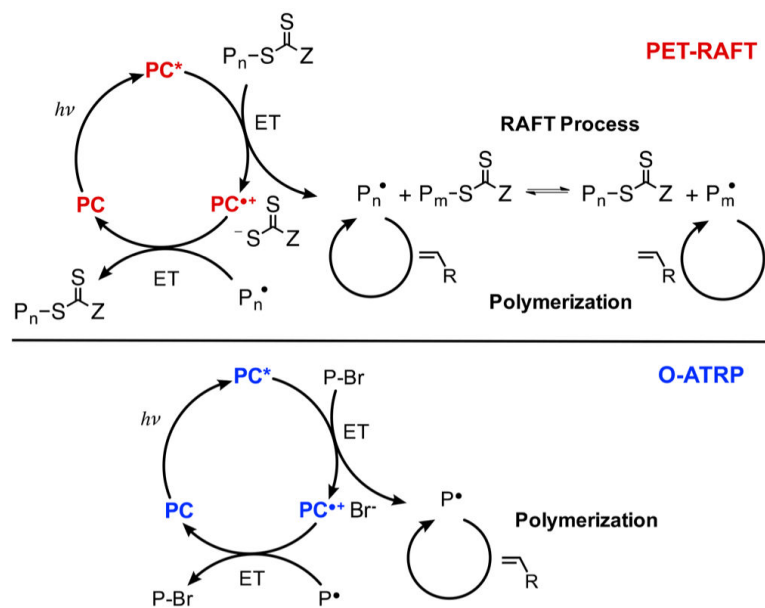


Figure 1. Proposed mechanisms of PET-RAFT (top) and O-ATRP (bottom), highlighting the similar role of the PC in each.

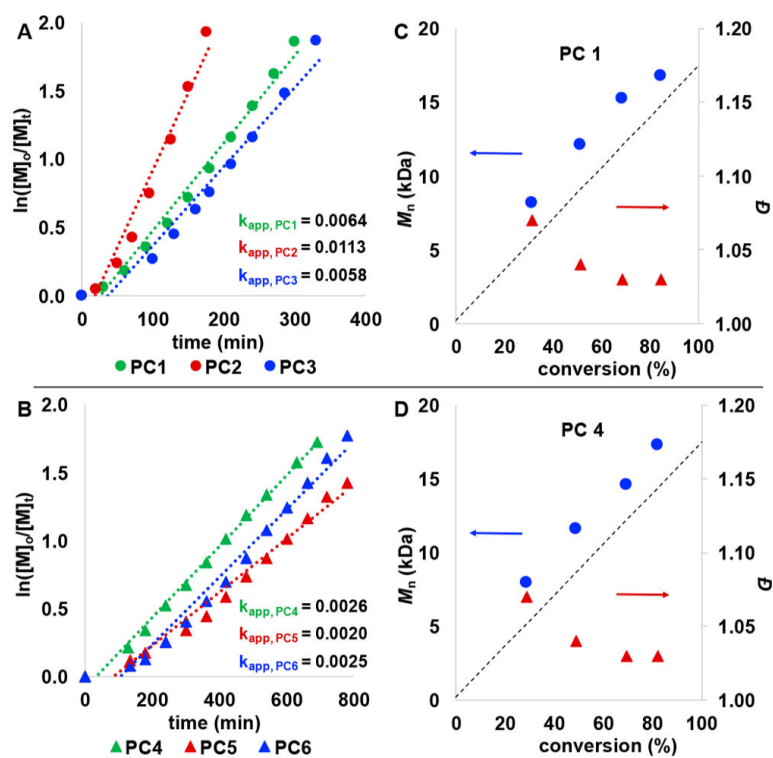


Figure 2. First-order kinetic analysis of the PET-RAFT polymerization of MA in DMSO using PCs 1–3 (A) and PCs 4–6 (B). Evolution of M_n and \bar{D} versus conversion using PC 1 (C) and PC 4 (D).

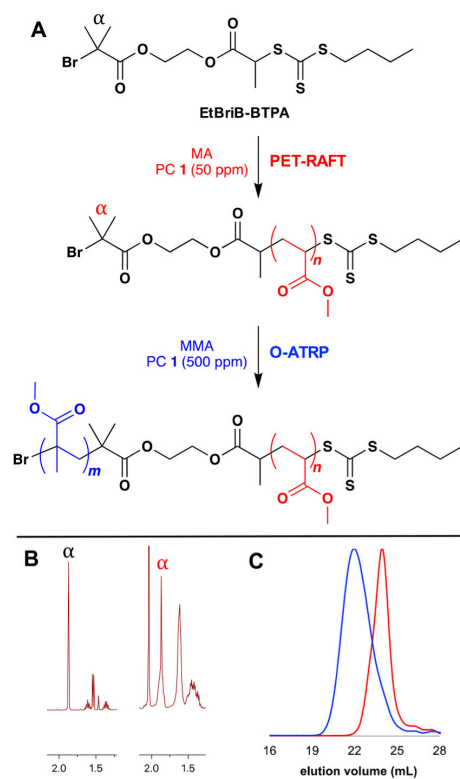
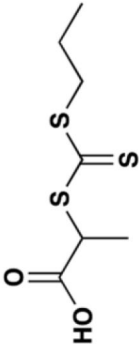


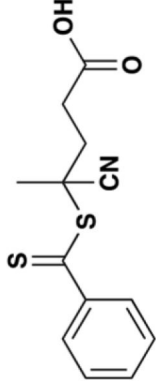
Figure 3. (A) Scheme of sequential PET-RAFT/O-ATRP copolymerization. (B) ¹H NMR spectra showing the indicated protons before (left) and after (right) the polymerization of MA. (C) GPC traces of PMA block (red) and PMA-*b*-PMMA copolymer (blue).

Table 1.
PET-RAFT Polymerizations of Various Monomers Using PCs 1 and 4 as Catalyst

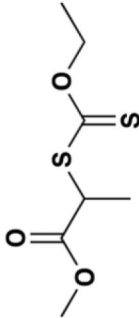
monomer	RAFT agent	time (h)	PC 1 (CT catalyst)				PC 4 (non-CT catalyst)			
			$M_{n,th}$ (kDa)	M_n (kDa) ^b	$(M_w/M_n)^c$	conv. (%) ^a	$M_{n,th}$ (kDa)	M_n (kDa) ^b	$(M_w/M_n)^c$	conv. (%) ^a
MA	BTPA	6	13.8	13.9	1.06	6	1.29	2.30	1.44	
MMA	CPADB	24	8.28	9.02	1.06	<1	-	-	-	
VAc	xanthate	20	5.93	8.62	1.12	<1	-	-	-	
DMA	BTPA	4	9.04	11.4	1.06	11	2.41	2.90	1.18	



BTPA



CPADB



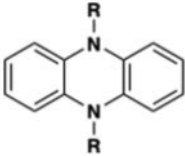
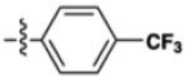
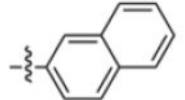
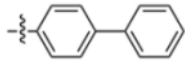
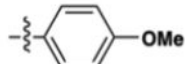
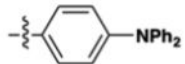

xanthate

^a Determined via ¹H NMR spectroscopy.

^b Determined via GPC using PMMA standards.

^c Determined via GPC. [Monomer]:[RAFT agent]:[PC] = 200:1:0.01 based on 0.5 mL of monomer; run in 0.5 mL of DMSO; 460 nm blue LED. See Table 2 for PC structures.

Table 2.
PET-RAFT Polymerizations of MA Using PCs 1–6 in Solvents of Varying Polarity

	DMSO	DMF	DMAc	EtOAc	THF	dioxane
Charge Transfer Catalysts						
PC 1, R = 	conv. ^a = 78.9% M_n^b = 13.9 ^c = 1.06	conv. = 68.8% M_n = 12.5 = 1.07	conv. = 85.4% M_n = 15.1 = 1.07	conv. = 80.0% M_n = 13.6 = 1.08	conv. = 90.7 % M_n = 13.8 = 1.16	conv. = 90.8% M_n = 18.4 = 1.06
PC 2, R = 	conv. = 87.2 % M_n = 17.3 = 1.08	conv. = 93.3% M_n = 19.1 = 1.06	conv. = 97.8% M_n = 19.7 = 1.08	conv. = 92.1 % M_n = 17.5 = 1.11	conv. = 97.0% M_n = 15.2 = 1.20	conv. = >99% M_n = 21.0 = 1.12
PC 3, R = 	conv. = 76.4% M_n = 15.9 = 1.07	conv. = 70.7% M_n = 13.4 = 1.07	conv. = 86.0% M_n = 17.0 = 1.06	conv. = 29.1% M_n = 7.4 = 1.16	conv. = 76.4% M_n = 13.4 = 1.07	conv. = 91.5% M_n = 19.4 = 1.08
Non-Charge Transfer Catalysts						
PC 4, R = 	conv. = 5.6% M_n = 2.3 = 1.44	conv. = 0%	conv. = 16.7% M_n = 3.7 = 1.25	conv. = 0%	conv. = 0%	conv. = 0%
PC 5, R = 	conv. = 8.3% M_n = 2.6 = 1.35	conv. = 0%	conv. = 29.6% M_n = 7.1 = 1.15	conv. = 0%	conv. = 10.7% M_n = 2.7 = 1.32	conv. = 0%
PC 6, R = 	conv. = 49.2% M_n = 10.7 = 1.05	conv. = 0%	conv. = 17.3% M_n = 5.6 = 1.17	conv. = 0%	conv. = 24.8% M_n = 5.4 = 1.20	conv. = 31.0% M_n = 8.2 = 1.15

^a Determined via ¹H NMR spectroscopy.

^b kDa, determined via GPC using PMMA standards.

^c M_w/M_n , determined via GPC. For all runs, [MA]:[BTPA]:[PC] = 200:1:0.01, based on 0.5 mL of MA; run in 0.5 mL of the indicated solvent (11 M); λ = 460 nm blue LED; irradiation time 6 h. Green denotes conv. > 50%. Yellow denotes 50% > conv. > 20%. Red denotes conv. < 20%.